JOURNAL OF VIROLOGY, Feb. 1992, p. 804–815
0022-538X/92/020804-12$02.00/0

Vol. 66, No. 2

Simian Virus 40 T-Antigen DNA Helicase Is a Hexamer Which Forms a Binary Complex during Bidirectional Unwinding from the Viral Origin of DNA Replication

RAINER WESSEL, JOHANNES SCHWEIZER,† AND HANS STAHL*
Fakultät für Biologie, Universität Konstanz, D-7750 Konstanz, Germany

Received 9 September 1991/Accepted 28 October 1991

The role of simian virus 40 (SV40) large tumor antigen (T antigen) as a DNA helicase at the replication fork was studied. We found that a T-antigen hexamer complex acts during the unidirectional unwinding of appropriate DNA substrates and is localized directly in the center of the fork, contacting the adjacent double strand as well as the emerging single strands. When bidirectional DNA unwinding, initiated at the viral origin of DNA replication, was analyzed, a larger T-antigen complex that is simultaneously active at both branch points of an unwinding bubble was observed. The size and shape of this helicase complex imply that the T-antigen dodecamer complex, assembled at the origin and active in the localized melting of duplex DNA, is subsequently also used to continue DNA unwinding bidirectionally. Then, however, the dodecamer complex does not split into two hexamer subunits that track along the DNA; rather, the DNA is threaded through the intact complex, with the concomitant extrusion of single-stranded loops.

The DNA of prokaryotic and eukaryotic cells as well as the DNA of many viruses is semiconservatively replicated following an apparently common molecular biological concept. According to this concept, DNA synthesis is performed bidirectionally in a semidiscontinuous fashion starting from defined points within the genome, conventionally called origins of DNA replication. The double-stranded DNA (dsDNA) at the origin is melted by an initiator protein, and this primary replication bubble is extended at its forks by a helicase, followed by the synthesis of daughter DNA (for reviews, see references 27 and 28).

In studies of the role of replicative helicases in the pathway of DNA replication, the simian virus 40 (SV40) large tumor antigen (T antigen) has proven to be very useful. Viral DNA replication, which takes place in the nuclei of monkey and human cells, requires T antigen in addition to numerous cellular factors (30, 50; for reviews, see references 15 and 48). T antigen specifically recognizes the pentanucleotide 5′-GAGGC-3′, present in four copies within the 64 bp of the SV40 core origin of DNA replication (11, 14, 52). In the presence of Mg^{2+} and ATP (Mg-ATP), it forms a double-hexamer complex, covering the complete core origin plus 12 bp in each direction (10, 31). This complex partially untwists the bound DNA region without the need for ATP hydrolysis (6, 37). From the melted origin region, T antigen can continue DNA unwinding bidirectionally in the presence of a single-stranded-DNA (ssDNA)-binding protein (SSB) and a topoisomerase, with hydrolysis of ATP being now essential (16, 35, 39).

From the SV40 replication studies and also from biochemical analyses, it is clear that T antigen is a DNA helicase that catalyzes both the localized melting of duplex DNA, with a high but not exclusive specificity for the SV40 origin (40), and also the processive unwinding of long stretches of dsDNA (46, 60). The two activities can be biochemically differentiated by their different response to some T-antigen-specific monoclonal antibodies and by their template requirements (40). For DNA melting, a minimum length of 50 to 60 bp of the dsDNA substrate (50 to 60 bp) is essential, most probably reflecting the size of the active T-antigen complex. In contrast, DNA unwinding of very short dsDNA regions (less than 20 bp) can be efficiently started by T antigen if the substrate contains a single-stranded 3′ extension of 5 to 10 nucleotides as an entry site (49, 60).

Confirming the role as the viral replication fork helicase (47, 59), DNA unwinding by T antigen proceeds at about the same rate as the rate of SV40 DNA replication (60). Moreover, in analogy to the prokaryotic systems, T antigen has also been found to associate with the DNA polymerase α-primase complex (17, 20, 44), though the 3′-to-5′ directionality of the T-antigen helicase movement differs from that of its prokaryotic counterparts and would place it on the template for the leading strand at the replication fork (opposite the position of the polymerase α-primase complex catalyzing SV40 lagging-strand DNA synthesis [22, 29, 60]). While these data demonstrate a T-antigen interaction with the replication machinery, more recent findings place it at the same time at the nuclear matrix, indicating that SV40 DNA replication proceeds at this structure (43). Therefore, a more detailed analysis of how T antigen combines its biochemical and structural functions during viral DNA replication is essential.

As mentioned above, local DNA denaturation at the SV40 origin apparently is initiated by the assembly of a T-antigen dodecamer complex. However, the size of the active helicase complex essential for the extension of this initial replication bubble is unknown, as is the relationship, if any, between this helicase complex and the initial T-antigen melting activity. We show that the basic DNA helicase of T antigen is a hexamer that is active during unidirectional unwinding, started from single strand/double strand (ss/ds) junctions of partially double-stranded DNA. Footprinting of the T-antigen helicase bound at an unwinding fork and electron microscopic analysis reveal that the hexamer complex is localized directly in the center of the fork, contacting the double strand as well as the emerging single strands. However, during bidirectional DNA unwinding, started from

* Corresponding author.
† Present address: Institut Pasteur, 75015 Paris, France.

the viral origin of DNA replication, a bilobed T-antigen helicase complex was observed operating simultaneously at both forks of an unwinding bubble, with the ssDNA looped out between. Thus, the double-hexamer complex forming at the viral replication origin becomes active as a processive helicase with two reactive centers subsequent to its initiation function. Since the helicase complex does not track along the DNA but rather the DNA is translocated in relation to the complex, our results provide direct support for a model of SV40 DNA replication in which the DNA is threaded through a fixed replication center.

MATERIALS AND METHODS

Reagents and enzymes. Nucleotides, restriction enzymes, endonuclease P1, exonuclease III, T4 polynucleotide kinase, and Klenow enzyme were purchased from Boehringer Mannheim, *Escherichia coli* SSB was from Pharmacia, Sequenase (version 2.0) was from U.S. Biochemical, and λ exonuclease was from Bethesda Research Laboratories. Radioactive nucleotides were from Amersham. Glutaraldehyde was from TAAB, formamide was from Fluka, and Bio-Gel A5m was from Bio-Rad. All other chemicals were purchased from Sigma. T antigen was isolated by the immunoaffinity procedure (46), using extracts from hybrid adenovirus-SV40-infected HeLa cells (33). The T-antigen-specific monoclonal antibody PAb 101 was prepared as described previously (47).

DNA constructs used as DNA helicase substrates. A partially double-stranded DNA containing a preformed fork (used in the experiments shown in Fig. 4 and 5) was prepared as follows. One strand, called here the 3′ strand and representing the fast-migrating strand of the denatured *Hin*dIII-*Pvu*II fragment (322 bases, *Hin*dIII site at the 5′ end) of plasmid pSVC4 (39) was prepared by elution after separation of the restriction fragment on a denaturing agarose gel. A 70-mer oligonucleotide with bases 31 to 70 complementary to bases 93 to 132 of the 3′ strand was annealed and elongated up to the end with Sequenase (used under conditions recommended by the supplier); this oligonucleotide was designated the 5′ strand of this substrate. As can be also seen from the schematic drawing in Fig. 4A, the substrate consists of a 132-bp double-stranded part carrying one blunt end at one side and two noncomplementary single strands of 190 bases (3′ strand) and 30 bases (5′ strand) at the other. The 5′ strand was radioactively labeled either at the 5′ end with [γ-^{32}P]dATP by T4 polynucleotide kinase prior to annealing or at the 3′ end by replacing dATP with [α-^{32}P]dATP during the elongation reaction with the Sequenase. The 3′ strand was labeled at its 5′ end also by using the T4 polynucleotide kinase and [γ-^{32}P]dATP (38).

A partially double-stranded M13 DNA (used in the experiments shown in Fig. 1) was created by annealing a 30-nucleotide primer complementary to nucleotides 6510 to 6539 of M13mp7 positive strand followed by elongation with Klenow enzyme in the presence of [α-^{32}P]dATP and nonradioactive dCTP by 8 nucleotides (for details, see reference 46).

A λ exonuclease-digested linearized pUC8 DNA (used in the experiments shown in Fig. 2 and 3) was prepared using 1.5 μg of *Sca*I-cleaved pUC8 DNA incubated for 10 s with 30 U of exonuclease as described previously (41). The procedure nearly quantitatively generated linear dsDNA molecules with single-stranded 3′ ends of a mean length of approximately 200 bases, as revealed by quantitative electron microscopy (EM) (for details, see reference 41).

The large fragment of *Ava*II-restricted pSVMO1 DNA (used for Fig. 6 and 7) (49) carrying the SV40 origin of replication 1.5 and 1.1 kbp from the ends was used in the origin-specific DNA unwinding experiments.

Nuclease protection experiments. ^{32}P-labeled DNA with a preformed fork (2.5 to 5 ng; see above) was incubated under standard helicase reaction conditions but in the presence of 2 mM adenylyl(γ,β-methylene)-diphosphonate (AMP-PCP) instead of ATP with indicated amounts of T antigen for 10 min at 37°C. Then 2.3 μg M13mp7 ssDNA was added, and incubation continued for additional 10 min. Nuclease digestion was started by addition of 105 to 135 U of exonuclease III and incubation for 10 min at 37°C or by addition of 5 to 10 μg of endonuclease P1 and incubation for 15 min at 37°C. Exonuclease III was used at limiting concentrations to prevent nonspecific degradation of the single-stranded part of the substrate. Reactions were stopped with 3 volumes of 50 mM EDTA–400 mM sodium acetate–0.5% sodium dodecyl sulfate (SDS). After phenol-chloroform treatment and ethanol precipitation, the DNA was dried and dissolved in 10 μl of 47% formamide–10 mM EDTA. The heat-denatured DNA was then analyzed on a 6% DNA sequencing gel, and the G+A Maxam-Gilbert-sequenced (32) ^{32}P-5′-end labeled 3′ strand was run alongside.

DNA helicase experiments. Standard DNA helicase assays were performed essentially as described previously (46). Briefly, 2.5 to 5 ng of ^{32}P-labeled DNA was incubated with 50 ng to 1 μg of T antigen in 20 mM Tris-HCl (pH 7.5)–4 mM $MgCl_2$–2 mM ATP at 37°C for the indicated times. Reaction products were analyzed by SDS-polyacrylamide gel electrophoresis and autoradiography (40); for quantitative analysis, the bands from the gel were sliced out and counted in a liquid scintillation counter as described elsewhere (60).

For EM, helicase assays contained 20 mM triethanolamine-HCl (pH 7.5) instead of Tris-HCl, lower concentrations (2 mM) of $MgCl_2$ (to avoid aggregation of T antigen that was observed at higher concentrations of free Mg^{2+}; unpublished observations), 80 mM NaCl (to inhibit nonspecific binding of T antigen), and 500 ng of *E. coli* SSB (to stabilize unwound single strands). Unwinding reactions were stopped by the addition of 0.1 volume of 1% glutaraldehyde in 20 mM triethanolamine-HCl (pH 7.5) and incubation for 15 min at 37°C. Unless indicated, free protein and glutaraldehyde were removed before use of the samples for EM by spin gel filtration using Bio-Gel A5m in 20 mM triethanolamine-HCl (pH 7.5) as described previously (58).

EM. Fixed samples were spread by using benzylalkyldimethylammonium chloride (BAC) (56) and processed for shadowing as described previously (58). Rotary shadowing was done with tungsten at an angle of 8° and controlled with a quartz crystal. The thickness of the tungsten layer was adjusted to 5 nm by the frequency change of the oscillating quartz crystal (500 Hz; see manual BB 800 048 BD, Balzers, Liechtenstein), and diameters of shadowed T-antigen helicase complexes were corrected for this value. For negative staining, samples were directly adsorbed for 1 min to airglow discharge-treated (15 s, 7 Pa, 110 V, 20 to 40 mA) carbon-coated grids and stained with 5% uranyl acetate for 15 to 20 s. Excess uranyl acetate was removed by blotting, and the grids were air dried. Micrographs were taken at a Hitachi H-7000, and tilt series were done with a Philips 400-T transmission electron microscope. Negatively stained tobacco mosaic virus was used as external length standard. Length measurements of pSVMO1 DNA for determination of the SV40 origin position were done on a CRP digitizer (Cybernetical Research & Production, Konstanz, Germany),

using magnified (100,000-fold) positives. Size measurements of T-antigen complexes were performed with a measuring lens using magnified (500,000-fold) positives. Diameters of individual complexes were calculated from four measurements, rotating the positive image clockwise after each measurement by an angle of 45°. The mass of T-antigen complexes was calculated from the mean diameter (determined from 50 complexes) of the negatively stained complexes, using the formula for mass determination of a spherical protein body: $M_r = d^3 \cdot \pi \cdot \rho \cdot N_A/6$, where M_r is the molecular weight, d is the mean diameter of the T-antigen complexes, ρ is the specific density of proteins ($1.33\ g \cdot cm^{-3}$ [25]), and N_A is Avogardo's number (6.022×10^{23} molecules per mol).

Sucrose gradient centrifugation. Gradients (4.5 ml) containing 5 to 20% sucrose in 10 mM Tris-HCl (pH 7.5)–0.1 mM ATP–0.1 mM $MgCl_2$–1 mM dithiothreitol –10% glycine were centrifuged in an SW55 rotor (Beckman) at 39,000 rpm for 19.5 h at 0°C and eluted in 250-μl fractions. Samples used for the T-antigen helicase assay and for the EM analysis were taken from the sucrose gradient fractions immediately after centrifugation and subsequently used for the respective assays. For calibration, gradients with marker proteins (hemoglobin, 4.3S, 65 kDa; aldolase, 7.4S, 158 kDa; catalase, 11.3S, 233 kDa ferritin, 17S, 440 kDa; and thyroglobulin, 19S, 669 kDa) were run in parallel under identical conditions.

RESULTS

Formation of helicase-active hexamers in the absence of DNA. Incubation of T antigen at 37°C in the presence of Mg-ATP but in the absence of DNA results in the formation of T-antigen oligomers with hexamers as the most specific complexes (31). Using a partially double-stranded DNA substrate, we found the T-antigen helicase still active after preincubation for 1 h under these conditions. At the same time, a sedimentation analysis disclosed a shift of the T-antigen protein (data not shown; 46) and of the DNA helicase activity from about 6S to 17S (Fig. 1C).

When analyzed by EM after negative staining with uranyl acetate, control T antigen (not preincubated with Mg-ATP) from the enzymatically active 6S peak (fraction 15 in Fig. 1C) appeared as 6- to 8-nm particles as would be expected for monomeric to dimeric forms (Fig. 1B). In contrast, micrographs of the 17S complexes manifested about 90% of T antigen in regular globular structures (Fig. 1A), with the rest of the complexes showing a smaller and heterogeneous size (not shown). The diameter of the main class of 17S complexes was 10.8 ± 0.7 nm (Table 1). A calculation of the M_r of a globular protein complex with this experimentally determined diameter (25; see also Materials and Methods) gives a mean value of 528,000. This is 6.4 times larger than the M_r of a T-antigen monomer (82,000) and implies that the helicase activity is associated with a hexameric form of T antigen, though the technique used here may not be sufficiently accurate to definitively distinguish between pentameric to heptameric forms of T antigen (see Discussion).

In the presence of ATP, free hexamers were stable at 37°C, whereas incubation of T antigen in the absence of Mg-ATP at 37°C for 1 h did not lead to detectable oligomerization and even destroyed preformed hexamers (data not shown). Moreover, incubation on ice in the presence of Mg-ATP did also not support the assembly of hexamer complexes, indicating that T antigen is converted on cooling into a state unable to form hexamers (data not shown; 31). Since of the various possible interactions, only hydrophobic interactions are impaired at low temperature (36), it is conceivable that they may have an important role in maintaining the hexameric structure of T antigen. Moreover, hydrophobic interactions could also explain the observed salt stability of the T-antigen helicase complex (60; unpublished observations).

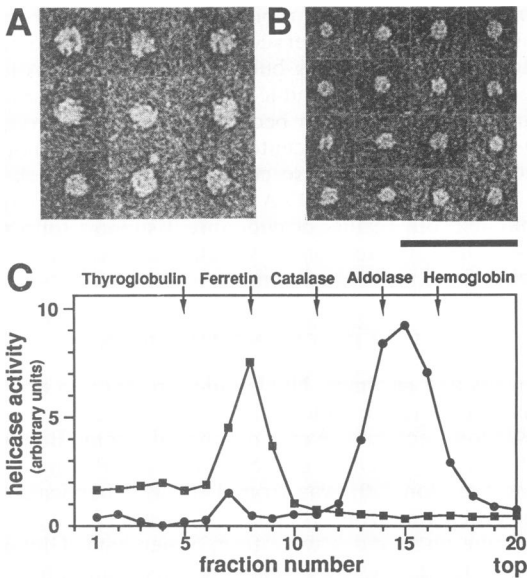

FIG. 1. DNA helicase activity in T-antigen hexamer complexes assembled in the absence of DNA. (A) EM analysis of T-antigen complexes taken from fraction 8 of the sucrose gradient shown in panel C, which was loaded with T antigen preincubated at 37°C in the presence of Mg-ATP but in the absence of DNA. Samples were fixed with glutaraldehyde, directly adsorbed to carbon-coated grids, and negatively stained (see Materials and Methods). The complexes shown represent about 90% of the T antigen. (B) EM analysis by negative staining of fraction 15 of the sucrose gradient shown in panel C and loaded with control T antigen (without preincubation). The shown complexes represent more than 90% of the T antigen. Bar, 50 nm. (C) A 60-μg sample of T antigen without preincubation (circles) or of T antigen incubated for 1 h at 37°C in a total volume of 100 μl in the presence of 1 mM Mg-ATP under otherwise standard helicase reaction conditions but in the absence of DNA (squares) was separated by sucrose gradient centrifugation (see Materials and Methods). Sedimentation was from right to left. Aliquots (10 μl) of collected fractions (250 μl) were tested for helicase activity under standard conditions, using 5 ng of partially double-stranded M13mp7 DNA as a substrate. Helicase reaction products were analyzed by gel electrophoresis and quantitated as described in Materials and Methods. The helicase activity was expressed as arbitrary units (1 U represents the unwinding of 0.2 fmol of partially double-stranded M13mp7 DNA).

TABLE 1. Dimensions of T-antigen helicase complexes[a]

Complexes	Mean diam (nm)[b]
Negatively stained free	10.8 ± 0.7
Tungsten shadowed free	13.4 ± 0.9
Tungsten shadowed fork bound	13.8 ± 0.8

[a] Free complexes were from the experiment shown in Fig. 1A; fork-bound complexes were from the experiment shown in Fig. 2A.

[b] Determined as described in Materials and Methods and calculated from 50 individual complexes of each type.

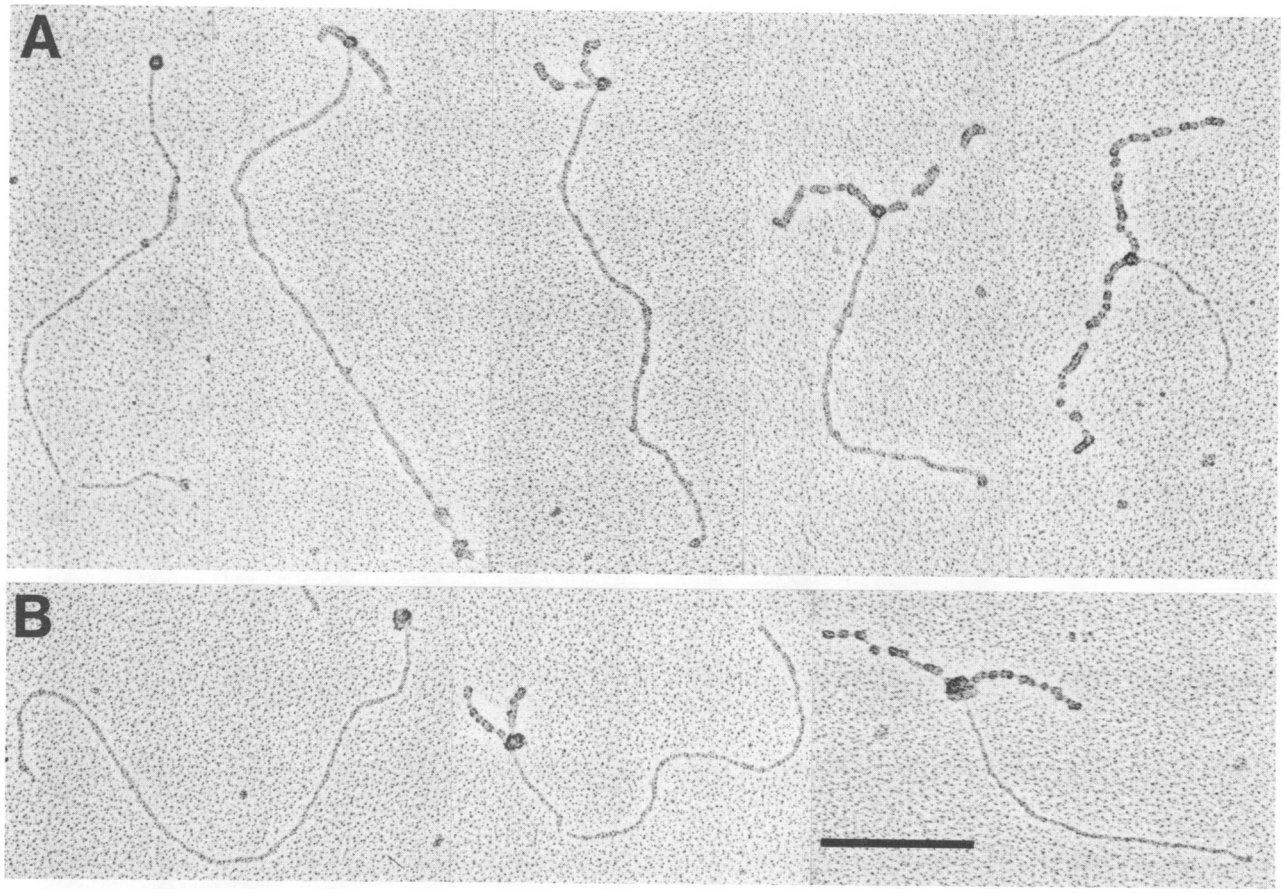

FIG. 2. EM demonstration of fork-bound T-antigen helicase complexes involved in progressive unidirectional DNA unwinding. (A) Linear pUC8 DNA (0.1 μg), containing 3′-extended single-stranded ends of ca. 200 bases, was incubated with 0.2 μg of T antigen for 15 min under helicase reaction conditions, and reaction products were processed for EM analysis (see Materials and Methods). Electron micrographs of progressively unwound DNA molecules are shown. A circular complex with high contrast is seen at the end (most probably at the ss/ds junction) of the first molecule and at the branch point of unwinding forks. Note that ssDNA, coated with *E. coli* SSB, is condensed about 2.7 times relative to duplex DNA, thus accounting for the discrepancy in the lengths of progressively unwound DNAs (27). (B) An unwinding reaction sample identical to that used for panel A was incubated with PAb 101 (500 ng) (23) after glutaraldehyde fixation and spin gel filtration for 15 min on ice. Sodium chloride (200 mM) was added; after fixation, a second spin gel filtration was performed to remove nonbound antibodies. Because of the presence of bound antibodies, the complexes at the branch points now appear larger and more amorphous than those without antibodies (shown in panel A). Bar, 200 nm.

Detection of an active T-antigen helicase complex in unwinding forks by EM. Preformed T-antigen hexamers may dissociate after isolation, and resulting substructures could give rise to the helicase activity detected in the 17S peak of Fig. 1. Therefore, we also analyzed individual T-antigen complexes actually involved in DNA unwinding by EM. A linearized plasmid DNA of 2.7 kb was used as a helicase substrate. The DNA contained small 3′-extended single-stranded regions at each end, created by a short incubation with the λ exonuclease, that served as highly efficient entry sites of the T-antigen helicase for unidirectional unwinding (60; for experimental details, see reference 41). After incubation of the DNA with T antigen for 15 min under helicase conditions in the presence of *E. coli* SSB, samples were fixed immediately with glutaraldehyde added directly to the unwinding reactions and spread for EM analysis. As has been reported before (16, 40), progressively unwound DNA molecules with two free single strands produced by the T-antigen helicase activity were obtained (Fig. 2). The denatured DNA is covered by the SSB and thus exceeds in diameter and contrast the nondenatured part of the DNA molecules. Since the 3′ single-stranded ends of the substrate served as highly efficient entry sites, T antigen apparently always started from the ends of the DNA molecules; unwinding bubbles resulting from internal starts (40) were not observed. The BAC spreading technique was used in combination with quartz crystal-controlled rotary tungsten shadowing, resulting in a good resolution of the different proteins in a nucleoprotein complex (58).

A protein knob with a higher contrast than the SSB was seen in the center of most unwinding forks (90%) and was believed to be T antigen, the only protein in addition to SSB present in the reaction sample (Fig. 2A). This conclusion was confirmed by staining of the protein-DNA complexes with a T-antigen-specific monoclonal antibody (PAb 101 [23]). Under these conditions, the protein knob appeared more amorphous and larger than in the preparations without antibodies (Fig. 2B). As the unwinding was carried out under stringent reaction conditions (80 mM salt), most DNA molecules were free of nonspecifically bound T antigen (49). From the panel of the nucleoprotein structures shown in Fig. 2A, it appears that the helicase complex first binds to the end

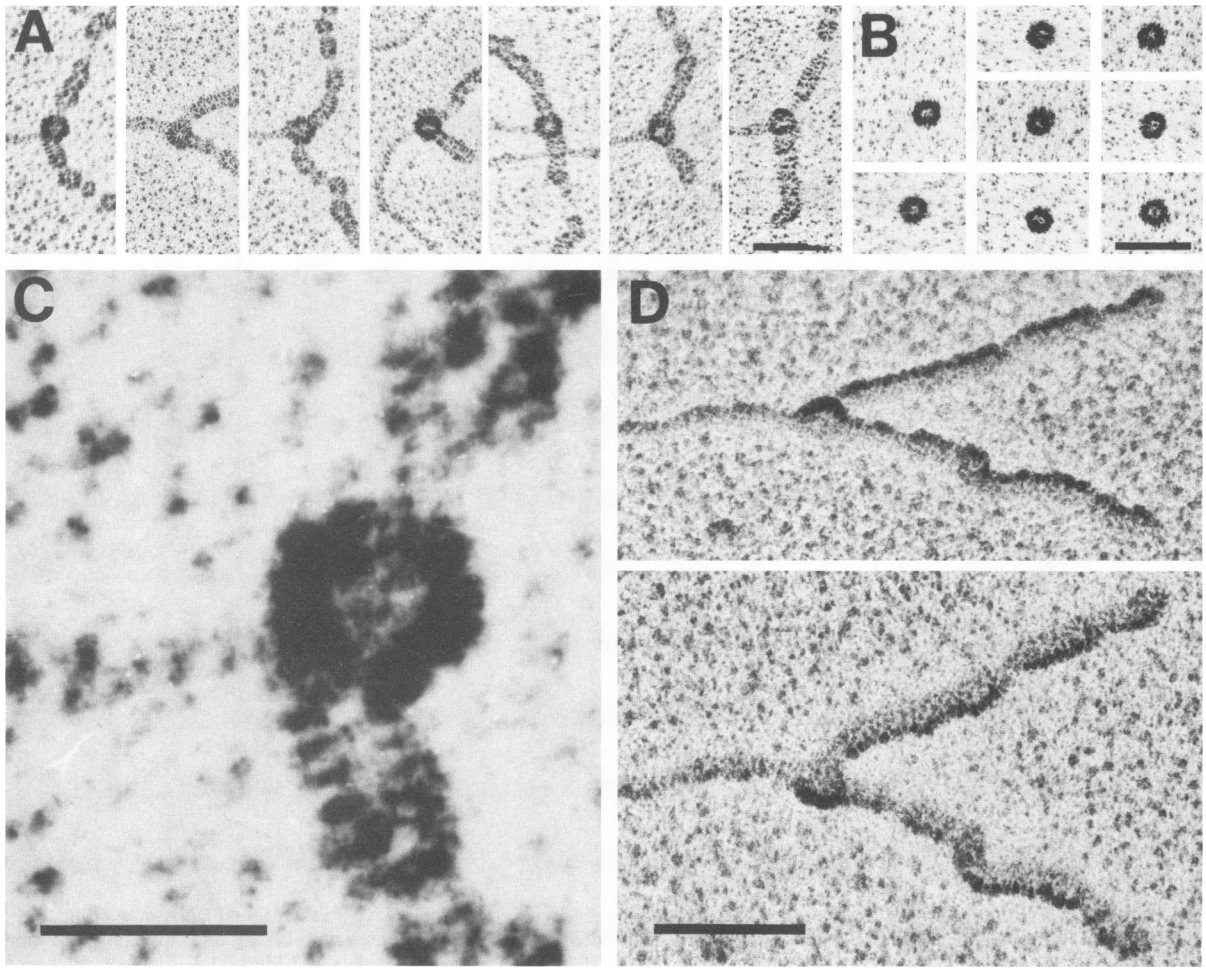

FIG. 3. Shape of fork-bound T-antigen helicase complexes. (A) Electron micrographs of the central part of DNA unwinding forks with the T-antigen helicase bound to adjacent ssDNA and dsDNA regions. DNA helicase substrate, helicase conditions, and EM procedures were identical to those used for Fig. 2. Note the circular pale spot in the center of each T-antigen complex, which likely reflects the spheric or hemispheric shape of the T-antigen complex shadowed at a small angle. Bar, 50 nm. (B) T-antigen complexes from the 17S fraction of Fig. 1 but spread by the BAC technique and rotary shadowed with tungsten exactly as done for panel A for visualization of T-antigen helicase complexes bound to unwinding forks. Bar, 50 nm. (C) Higher magnification of the first unwinding fork shown in panel A. Bar, 20 nm. (D) An unwinding fork (the second one shown in panel A) photographed under different tilt angles (upper, +60°; lower, −40°). Note the hemispheric appearance of the fork-bound T-antigen complex with a height depending on the tilt angle. Bar, 50 nm.

of the DNA molecules, most probably at the ss/ds junction, and then processively invades the double-stranded section. Fork-bound T antigen complexes remained stable after treatment of unwinding intermediates with salt (500 mM) or EDTA (1 mM) before fixation with glutaraldehyde but were not observed when unwinding reactions were run in the absence of Mg-ATP (data not shown).

The T-antigen helicase was always bound directly to the center of the fork, apparently interacting with all three strands. At high magnification (Fig. 3A and C), helicase complexes from different unwinding intermediates always were identical and appeared as a circular dark spot with a pale center, which likely reflects the micrographic appearance of hemispheric or spheric complexes after rotary shadowing at a small angle. This assumption was confirmed by a tilt series of electron micrographs, which gives more information about the three-dimensional shape (Fig. 3D). Complexes delineated at an angle of −40° or +60° now appeared as distinct caps with a height resembling the angular profile. Size measurements of fork-bound T-antigen complexes (Table 1) revealed diameters ranging from 12.7 to 14.9 nm, with an average value of 13.8 ± 0.8 nm. This size is identical to that of the 17S hexameric complexes from the sucrose gradient of Fig. 1 prepared by the BAC spreading method (Fig. 3B) and shows that the fork-bound T-antigen complexes are also hexamers (Table 1).

Footprint of the T-antigen DNA helicase bound at an unwinding fork. In the unwinding intermediates of Fig. 2 and 3, helicase complexes appeared always bound directly to the center of the fork, apparently interacting with all three strands. To map the position of the T-antigen helicase within the fork more precisely, we tried footprinting experiments. We used a partially double-stranded DNA of known sequence as a helicase substrate that consisted of a 132-bp duplex region with two noncomplementary single strands of 190 and 30 bases at one side (Fig. 4A). The predicted structure of the DNA construct with this preformed unwinding fork was confirmed by proving the accessibility of the

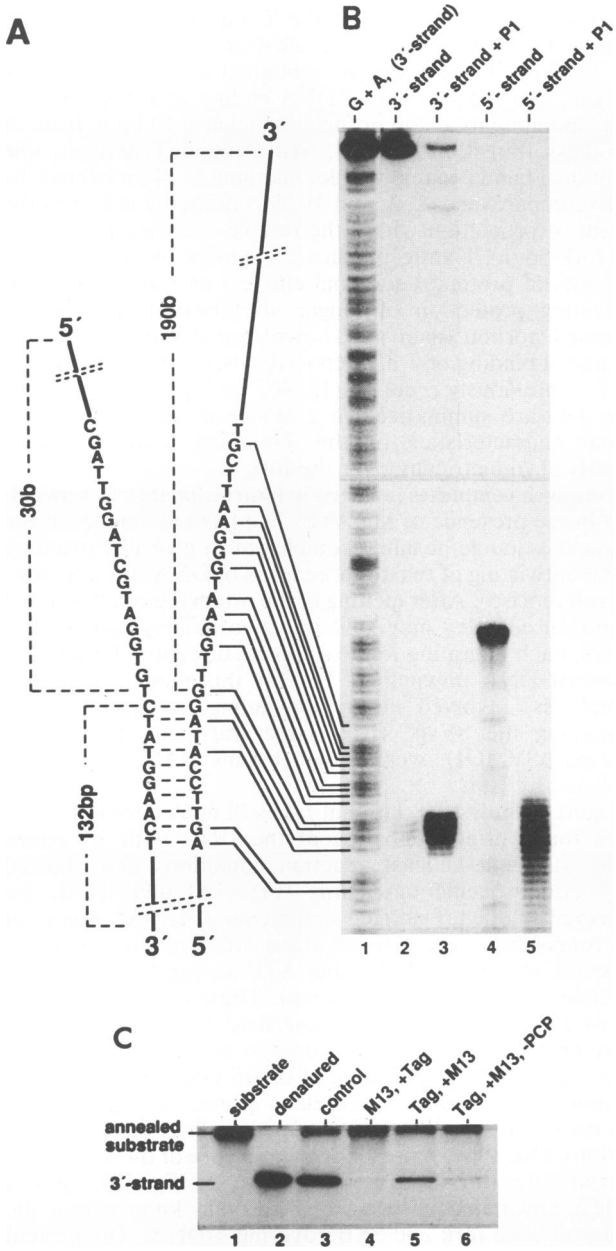

FIG. 4. Construction and function of a T-antigen DNA helicase substrate containing a preformed unwinding fork. (A) Schematic drawing of the DNA helicase substrate used in the nuclease protection experiments. Individual strands are referred to as the 3 strand and 5′ strand according to their 3′ and 5′ single-stranded ends, respectively. The lengths of the double-stranded part and of the single-stranded ends as well as the DNA sequence in the vicinity of the fork are indicated. Single-stranded regions of the DNA construct were analyzed by their sensitivity to nuclease P1 (B). The DNA was labeled either at the 5′ end of the 3′ strand (lanes 1 to 3) or at the 3′ end of the 5′ strand (lanes 4 and 5) and subjected either to a Maxam-Gilbert G+A reaction (lane 1) or a nuclease P1 (10 μg) digestion (lanes 3 and 5). Reaction products were analyzed by autoradiography after separation on a 6% DNA sequencing gel in comparison with the untreated 3′ strand (lane 2) and 5′ strand (lane 4). (For experimental details, see Materials and Methods.) (C) Analysis by polyacrylamide gel electrophoresis and autoradiography of unwinding of the substrate DNA shown in panel B by T antigen. Binding of T antigen (Tag; 0.3 μg) to the substrate DNA (2.5 ng; labeled at the 5′ end of the 3′ strand; specific activity, 700 Bq/ng), was allowed only during preincubation under helicase reaction conditions but in the presence of AMP-PCP (2 mM) instead of ATP at 37°C for 15 min. After preincubation, excess amounts (2.3 μg) of M13 ssDNA and 4 mM ATP were added, and the incubation was continued for additional 30 min (lane 5). Reactions were performed in the absence of M13 DNA (control; lane 3), with M13 DNA present during the preincubation step (lane 4), in the absence of AMP-PCP during preincubation, or with AMP-PCP added after preincubation (lane 6). Analysis of the native (lane 1) and denatured (lane 2) substrate DNA is also shown.

overhanging single strands by the single-strand-specific nuclease P1. After digestion, the radioactively labeled substrate was examined on a sequencing gel next to a G+A sequencing ladder, showing that nuclease P1 removed essentially all of the overhanging single strands (Fig. 4A, lane 3 and 5). Moreover, using denatured substrate DNA as a control, we obtained completely digested DNA under the same conditions (data not shown). The double-stranded part of the DNA construct was established by its sensitivity to double-strand-specific 3′ exonuclease III (see below).

The DNA substrate was efficiently unwound by T antigen under standard DNA helicase conditions (Fig. 4B, lane 3). ssDNA (M13 DNA) was an effective inhibitor of the unwinding reaction because it competed with the substrate DNA for T-antigen binding (lane 4) (60). However, preincubation of the substrate DNA with T antigen in the presence of the nonhydrolyzable ATP analog AMP-PCP allowed the formation of a T-antigen preinitiation complex, which, after addition of ATP, performed the reaction even in the presence of M13 ssDNA (lane 5). Thus, stalled T-antigen helicase complexes were bound to the preformed unwinding forks, a reaction that was strongly stimulated by AMP-PCP. In fact, 1 mM ATP-PCP did not inhibit the T-antigen ATPase or DNA helicase activities during the subsequent unwinding step after addition of 2 mM ATP but was slightly stimulatory, most probably by promotion of suitable complex formation (data not shown; 7).

The exact position of T antigen at the preformed unwinding fork was investigated by DNase protection experiments (Fig. 5). The interaction of T antigen with each of the two single strands was analyzed by protection against degradation by nuclease P1 (Fig. 5A and B). After preincubation of the DNA substrate (labeled at either strand) with T antigen and Mg-AMP-PCP under helicase reaction conditions, P1 digestion was performed in the presence of an excess of M13 DNA to remove nonspecifically bound T antigen. The experiments performed in the absence of T antigen again showed that digestion ceased on both strands near the ss/ds border (lanes 2 and 3 in Fig. 5A and lane 1 in Fig. 5B). Only in the presence of T antigen, P1 digestion of both overhanging single strands resulted in additional sharp bands that could be mapped 16 to 17 nucleotides in front of the fork on the 5′-extended single strand (Fig. 5A, lanes 5 and 6) and 9 to 10 nucleotides on the 3′-extended single strand (Fig. 5B, lanes 2 to 4). Nuclease protection was stimulated by, though not absolutely dependent on, Mg-AMP-PCP (compare lanes 4 and 5 in Fig. 5A), which is consistent with similar observations concerning the ATP-independent formation of a T-antigen unwinding complex at the SV40 origin (31). The percentage of the protected DNA molecules was low but similar to that of molecules unwound in the presence of M13 ssDNA after preincubation with PCP (Fig. 4B), indicating that the protection was really due to fork bound T-antigen helicase complexes.

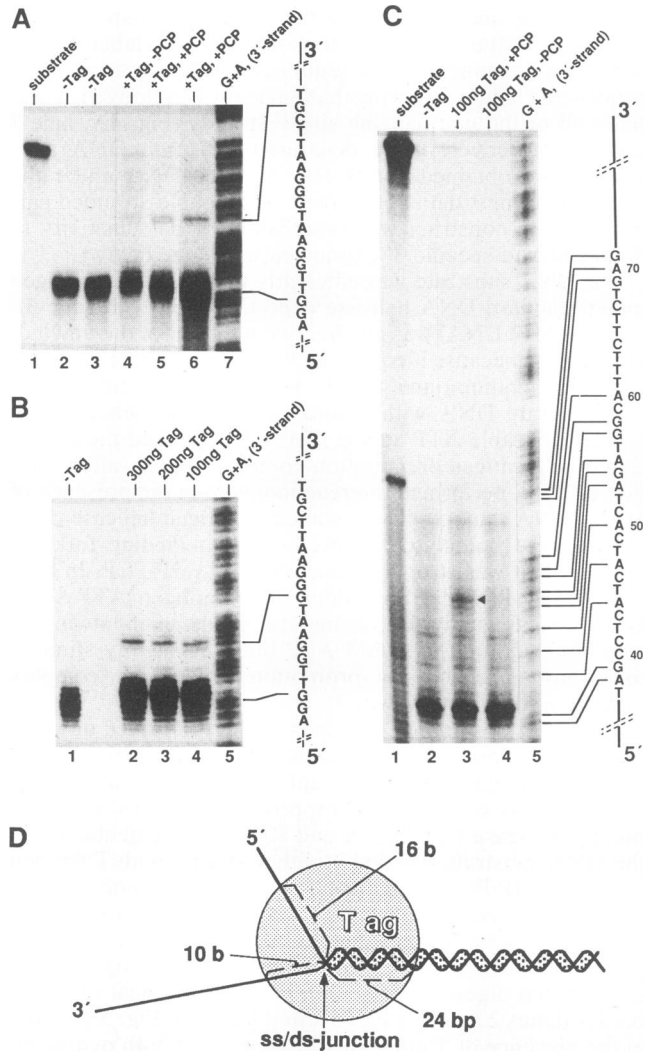

FIG. 5. Footprint of the T-antigen helicase complex bound at a preformed unwinding fork. (A) P1 protection of the 5′ strand of the DNA substrate shown in Fig. 4A. DNA (2.5 ng; see Fig. 1A) labeled at the 3′ end of the 5′ strand (lane 1) was preincubated without (lanes 2 and 3, showing identical experiments) or with (lanes 4–6) T antigen (Tag; 200 ng) under standard helicase reaction conditions but in the presence of 2 mM AMP-PCP instead of ATP for 15 min at 37°C (lanes 2, 3, 5, and 6) or with no nucleotide (lane 4). After a further incubation period of 15 min in the presence of 2.3 μg of M13 ssDNA, endonuclease P1 digestion and analysis of the resulting products on a 6% polyacrylamide sequencing gel were done as described in the legend to Fig. 4A and Materials and Methods. The experiment in lane 6 is shown as an overexposure (twofold) of the autoradiogram. A Maxam-Gilbert G+A sequencing reaction of the complementary 5′-end-labeled 3′ strand was analyzed in parallel as a size marker (lane 7). Positions of the ss/ds junction (first single-stranded nucleotide) and of the band induced by T-antigen protection are indicated and are aligned with the sequence of the 3′ strand. (B) P1 protection of the 3′ strand labeled at the 5′ end (see Materials and Methods). Experimental conditions were the same as for panel A. Lanes: 1 to 4, no T antigen or 0.3, 0.2, and 0.1 μg of T antigen, respectively, added during the preincubation step in the presence of AMP-PCP; 5, Maxam-Gilbert G+A sequencing reaction of the 3′ strand, with alignment of the positions of the ss/ds junction and of the band protected by T antigen to its DNA sequence. (C) Exonuclease III protection of the 5′ strand. The substrate DNA (lane 1) was labeled at the 5′ end of the 5′ strand (the intermediate band represents some labeled nonannealed 70-mer oligonucleotide used for the construction of the substrate DNA; see Materials and Methods). Preincubation of the DNA with T antigen, exonuclease III digestion, and analysis of the resulting products were done as described in Materials and Methods and for panel A. Preincubations were performed without T antigen (lane 2) or with 0.1 μg of T antigen in the presence (lane 3; the triangle marks the band induced by T-antigen protection) or absence (lane 4) of AMP-PCP. A Maxam-Gilbert G+A sequencing reaction of the 5′-end-labeled 3′ strand was run in parallel as a size marker; the related DNA sequence is shown (lane 5). (D) Model showing the localization of the helicase complex at the unwinding fork. Numbers indicate the lengths (in bases or base pairs) of DNA strands protected by T antigen.

To analyze the binding of the T-antigen helicase to the double-stranded portion of the substrate, we used exonuclease III (Fig. 5C). The results, obtained in the absence of T antigen, showed a smear of DNA ending at a defined band corresponding to a stop of the exonuclease 10 bp in front of the ds/ss transition (lane 2). With bound T antigen, one additional band became visible, mapping at 24 bp behind the fork (compare lanes 2, 3, and 4). This probably indicates the extent of protection within the double-stranded portion by the fork-bound T-antigen helicase complex. With increasing amounts of protein, additional clusters of bands appeared, indicating protection of longer stretches of the double-stranded portion (data not shown), most probably due to enhanced binding of T antigen to dsDNA in the presence of ATP as previously reported (12, 40). In Fig. 5D, the protection data are summarized in a model showing the dimensional characteristics of the T-antigen helicase placed slightly asymmetrically over the fork.

T-antigen complexes involved in bidirectional DNA unwinding. In the presence of Mg-ATP, T antigen assembles at the origin as a double-hexamer complex most probably resulting in the untwisting of two to three turns of DNA (for a review, see reference 5). After melting of the origin region, this initial T-antigen complex may split into two helicase-active hexamers, each migrating to the opposite direction during bidirectional DNA unwinding. To test this model, T-antigen complexes, involved in the unwinding of plasmid DNA containing the SV40 origin (large fragment of *Ava*II-restricted pSVMO1), were spread by the BAC method and analyzed by EM.

Figure 6 shows the different types of nucleoprotein structures found after incubation of the DNA with T antigen under stringent helicase reaction conditions that allowed only origin-specific unwinding (Fig. 7A) (49). First, we observed bilobed T-antigen complexes (Fig. 6B) bound at the origin that were also obtained after incubation in the presence of a nonhydrolyzable ATP analog but not in the absence of ATP (data not shown). These origin complexes appeared identical to those described by others (10) and most probably represent the double hexamers apparently involved in the initial melting of origin DNA (31).

About 5% of the DNA molecules scored were found to be unwinding intermediates of two apparently different conformations. One type, representing about 75% of the unwinding intermediates (for a statistical analysis, see Fig. 7B), showed a clear unwinding bubble with a protein knob within the center of each fork and SSB covering ssDNA. The protein complex in the center of the forks was determined to have the same dimensions described above for the T-antigen helicase (Fig. 2 and 3) and could also be immunologically stained by PAb 101 (data not shown). The other type, representing about 25% of unwinding intermediates, consists

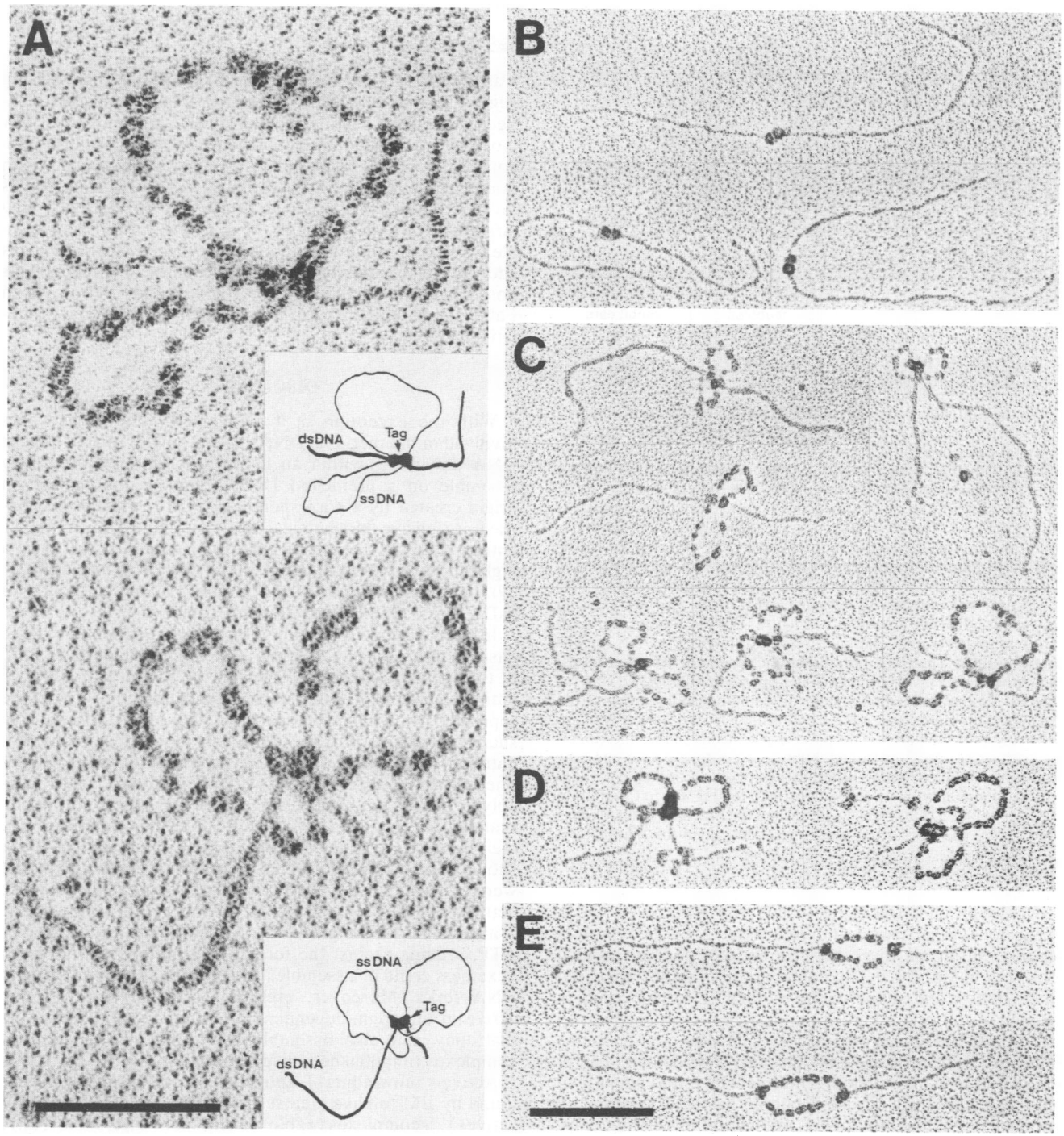

FIG. 6. Electron micrographs of unwinding intermediates started from the SV40 origin of DNA replication. (A) The large fragment of *Ava*II-restricted pSVMO1 DNA (0.1 μg), containing the origin of replication 1.1 and 1.5 kbp from the ends, was incubated with T antigen (1 μg) under origin-specific helicase reaction conditions (see Materials and Methods) for 15 min, spread by the BAC method, and processed for EM as described for Fig. 2. Shown are high magnifications of one type of unwinding intermediate structure, containing single-stranded loops (rabbit ears). Bar, 100 nm. Inserts show model drawings deduced from the micrographs. The bilobed protein complex in the center of the unwinding intermediates, connecting both forks and resulting in the looping out of the DNA single strands, has been identified as T antigen (Tag) (see panel D). (B) Micrographs from the reaction mixture used for panel A, showing bilobed T-antigen complexes bound at the origin position. (C) Micrographs of the type (rabbit ears-containing structures) shown in panel A, representing different stages of the unwinding process. The type of complexes shown comprises about 25% of unwinding intermediates obtained (for statistical analysis, see Fig. 7). (D) Micrographs representing unwinding intermediates obtained after a preincubation of T antigen with the monoclonal antibody PAb 101 (0.7 μg) for 15 min on ice before the onset of the helicase reaction by the addition of the large pSVMO1 *Ava*II fragment. Helicase reaction conditions and processing of unwinding intermediates were otherwise exactly as described for panel A. The rabbit ears-containing structures shown comprise about 75% of unwinding intermediates obtained under these conditions. Note the large size and amorphous shape (due to bound antibodies) of the protein complex connecting both forks of each molecule. (E) Micrographs of the helicase reaction mixture used in panel A but incubated in the presence of 10 mM EDTA at 0°C for 5 min prior to fixation with glutaraldehyde. The main species of unwinding intermediates obtained under this conditions are fully expanded unwinding bubbles which arose by bidirectional unwinding started from the origin (see also Fig. 7A). Note the individual T-antigen complexes bound at the branch points of both forks of each molecule. Bar, 200 nm.

A

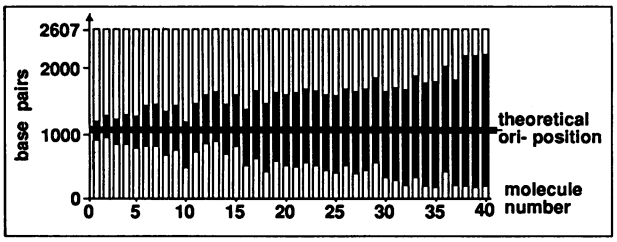

B

reaction conditions	structure of unwinding intermediates	
	bubbles	rabbit ears
standard reaction conditions	75%	25%
EDTA before fixation	96%	4%
antibody before reaction start	23%	77%

FIG. 7. Statistical analysis of unwinding intermediates obtained with substrate DNA containing the SV40 replication origin. (A) T-antigen-catalyzed bidirectional DNA unwinding from the origin of replication. A 0.1-μg sample of the large *Ava*II fragment (2,607 bp) of the pSVMO1 plasmid that contained the origin of replication 1.1 and 1.5 kbp from the ends was used. Helicase reaction conditions and EM analysis were exactly as described for Fig. 6. No differences for the origin specificity were observed in the different protocols used. Unwinding intermediates were photographed, and the lengths of the dsDNA arms were measured on a digitizing board. The shorter arm was taken to be the one closest to the replication origin and was placed at the bottom of the figure. White columns represent dsDNA regions; black columns represent unwound ssDNA regions coated by SSB. The thick horizontal line represents the theoretical origin position. The linearized 4,360-bp plasmid pBR322 was included as an internal length standard; the standard deviation of the length measurements was 3.5%. (B) Frequency of different types of unwinding intermediates. The percentage of unwinding intermediates with expanded unwinding bubbles or rabbit ears-containing structures, obtained under different protocols, is indicated. Standard reaction conditions were as described for Fig. 6A to C; addition of EDTA before fixation was as described for Fig. 6 E; antibody was added before the start of the reaction as described for Fig. 6D.

of two loops of ssDNA (again covered with SSB) which appear to emerge from, and return to, a bilobed protein complex, sitting on the otherwise entirely double-stranded DNA (Fig. 6A and C). The central protein knobs appeared similar in size and shape to the bilobed T antigen complex obtained at the origin before the initiation of unwinding. In fact, it could be immunologically stained after fixation with a T-antigen-specific monoclonal antibody (see below). Therefore, in this kind of unwinding intermediates, the two branch points of each single-stranded bubble are held together by the internal T-antigen complex. Individual unwinding complexes had single-stranded loops of different lengths ("rabbit ears") representing different stages of unwinding. When the unwinding reaction was stopped with EDTA before fixation, unwinding intermediates with single-stranded loops were found to be drastically reduced (4% of controls), and the fraction of unwinding intermediates with completely unfolded bubbles were accordingly increased (Fig. 7B).

The percentage of unwinding intermediates with the rabbit ears structures was significantly increased when T antigen was preincubated with the monoclonal antibody PAb 101 before the unwinding reaction (Fig. 6D). In this case, 77% of unwinding intermediates contained rabbit ears. The T-antigen knobs holding together the branch points were somewhat larger and amorphous because of bound antibodies (Fig. 6D). In addition, when T antigen was preincubated with PAb 101, the percentage of unwinding intermediates also was considerably higher (at least fivefold; data not shown), suggesting a more efficient formation of helicase-active T-antigen complexes. Similar data were obtained previously by biochemical unwinding experiments using an SV40 origin-containing DNA fragment as a substrate but also with non-origin-containing DNA substrates (40). Because of its bivalent nature, one molecule of the PAb 101 antibody may interact with both hexamers of a T-antigen initiation complex and cross-link them, especially since PAb 101 was added prior to the formation of helicase complexes. This possibility was confirmed in a previous study (40) in which Fab fragments of PAb 101 were shown to lose their stimulating activity.

DISCUSSION

With the exception of T antigen, all known helicases involved in bidirectional DNA replication are unable to start DNA unwinding within an intact dsDNA substrate. They assemble on a premelted DNA region at the replication origin created by a corresponding initiator protein. In contrast, extensive biochemical analyses have shown that T antigen catalyzes both the melting of duplex DNA, with a high but not exclusive specificity for the SV40 origin (6, 37, 39), and the processive unwinding of long stretches of dsDNA as a true DNA helicase (22, 60).

In this study, we first characterized the composition of the basic T-antigen DNA helicase. After preincubation at 37°C in the presence of Mg-ATP but in the absence of DNA, T antigen assembled into stable complexes that could be separated as a discrete species sedimenting at 17S in a sucrose gradient. Sedimentation behavior and size determination by EM, using the method of negative staining, identified the 17S complexes as T-antigen multimers, most probably hexamers. Our conclusions were strongly confirmed by scanning transmission EM, which allowed more precise size measurements (31). By this method, T antigen has also been shown under the same conditions to form free hexamers that were, however, not reported to possess DNA helicase activity, in contrast to the results presented here. Free T-antigen hexamers proved to be stable in the presence of ATP, arguing against the formal possibility that preformed hexamers could disassemble and subsequently reassemble at DNA forks. Moreover, preformed complexes were also active in an origin-dependent unwinding assay, indicating that they can also assemble into functional dodecamer complexes (unpublished observations).

Actively unwinding T-antigen helicase complexes were found by EM to have almost the same size as the (helicase-active) 17S complexes (Table 1). The small difference, if any, may result from the DNA contained within the fork-bound complexes. The EM analysis of unwinding intermediates therefore confirms that the hexamer complex indeed resembles the helicase-active T-antigen form. Actually unwinding helicase complexes were bound directly in the center of unwinding forks, which was further confined by footprinting experiments. The data clearly demonstrate that the T-antigen helicase complex interacts with all three strands of a fork, protecting about 10 and 16 bases of the protruding 3′ and 5′ single strands, respectively, and about 24 bp of the double-stranded portion ahead of the fork. Even though T antigen interacts with a longer stretch of the single-stranded 5′ strand, this does not necessarily contradict the earlier biochemical findings that the interaction with the 3′ strand probably determines the directionality of helicase movement (22, 60). Our data are also consistent with the concept that T

antigen, specifically interacting with the 3′ strand, simultaneously forms close contacts with the DNA polymerase-primase complex at the 5′ strand of the replication fork. The protected DNA within the fork most likely also reflects dimensions of the T-antigen helicase complex, although we cannot exclude the possibility that the nucleases used stopped some nucleotides in front of the helicase complex as a result of steric hindrance. We note, however, that T antigen was found in this study to protect a length of the 3′-extended single strand similar to that required for an efficient start of the T-antigen helicase at partially double-stranded DNA (5 to 10 nucleotides [60]). The size of the helicase complex deduced from the nuclease protection data and from EM analysis amounts to approximately half of that determined for the dodecamer complex formed at the origin and covering about 84 bp (12, 31). Taken together, our data strongly indicate that a hexameric complex represents the basic T-antigen helicase. Interestingly, two helicases of *E. coli*, the DnaB and Rho proteins, are also active as hexamers (4, 8, 19), and it may be speculated that this property has been conserved for functional reasons during evolution.

At 37°C and in the presence of ATP, T antigen assembles at the SV40 origin as a double-hexamer complex which is assumed to perform local DNA melting (31). Interestingly, this double-hexamer complex is shown here to bind simultaneously to both forks of unwinding bubbles that were formed during bidirectional DNA unwinding started from the origin. As the most plausible explanation for the generation of these structures, we propose that the double-hexamer complex, assembled at the SV40 origin and used for the initial melting, subsequently becomes also active in bidirectional DNA unwinding. Since unwinding is performed at two unwinding centers within the bilobed complex, the basic helicase again is a T-antigen hexamer, as shown for unidirectional unwinding with partially double-stranded substrates. The correct orientation within the bilobed complex with regard to the unwinding direction of the helicase subunits may be ensured by the 27-bp inverted repeat at the origin during the T-antigen assembly process.

Under standard reaction conditions, approximately 75% of the unwinding intermediates showed a clear unfolded unwinding bubble with a T-antigen hexamer in the center of each fork. We do not know whether this structure resembles real unwinding intermediates resulting from potential splitting of the bilobed T-antigen complex at later stages in the unwinding reaction or whether it is an artifact of the preparation. PAb 101, bound to T antigen before the onset of the unwinding reaction, apparently stimulates the formation of or stabilizes binary helicase complexes, since in the presence of the antibodies, the rabbit ears-containing structures are the major unwinding intermediates. Bound antibodies may simulate in vivo conditions in which the T-antigen unwinding complex seems to be bound to structural elements (nuclear matrix), possibly resulting in a stabilization and also stimulation of the replication complex (see below).

EDTA treatment seems to disrupt the double-hexamer complex, whereas single T-antigen hexamers, bound to the center of unwinding forks, appear to remain stably bound to DNA under these conditions. Therefore, different mechanisms must be involved in the formation of single T-antigen hexamers and the association of dodecamer complexes at the origin. Whereas hydrophobic interactions seem to be involved in the formation of hexamer complexes (see Results), magnesium-mediated protein-protein interactions of T-antigen molecules have been reported to induce DNA loops, and it seems that similar interactions are also important during bidirectional DNA unwinding (41). However, EDTA may also affect some other metal ion such as zinc that may be bound by the zinc finger region of T antigen (30a).

DNA unwinding starting from an origin of replication and continued bidirectionally by one and the same helicase complex acting simultaneously at both forks provides direct support for previously proposed models of DNA replication in which the DNA moves while the replication machine remains at a fixed site. Moreover, the DNA helicase could function as an organizer of the replication machine and at the same time could fix it to the nuclear scaffold, possibly arranged in replication centers with multiple replication forks as has been suggested recently for viral and cellular DNA (13, 24, 34, 54). Accordingly, the (transient) binding of replication origins, as well as replicating DNA, to structural elements has been described (18, 21, 26, 55; for a review, see reference 53), and during a lytic infection, a subfraction of T antigen is bound to the nuclear matrix and has been suggested to be actively involved in SV40 DNA replication (42, 43, 57). In this context, it is also interesting to note the frequent colocalization of detected replication origins with matrix attachment sites (1–3, 9).

Finally, the simultaneous binding of the helicase complex to both branch points of a replication bubble would guarantee a synchronous progression of related forks. Indeed, T antigen has been reported to be associated with replicating intermediate SV40 chromatin particularly distinguished by synchronously moving forks (45, 51). The association of forks in a topologically closed replicating DNA molecule would also prevent an accumulation of torsional strain in replicated sections. An extensive catenation of daughter strands could thus be avoided.

ACKNOWLEDGMENTS

We thank R. Knippers for continuing support and helpful discussions, K. Mendgen for making available the Hitachi H-7000, and H. Müller for help with the tilt series on the Philips 400 T transmission electron microscope. We also thank W. Ruyechan for critical reading of the manuscript and T. Kapitza for excellent technical assistance.

This work was supported by the Deutsche Forschungsgemeinschaft.

REFERENCES

1. **Amati, B., and S. M. Gasser.** 1988. Chromosomal ARS and CEN elements bind specifically to the yeast nuclear scaffold. cell **54**:967–978.
2. **Amati, B., and S. M. Gasser.** 1990. Drosophila scaffold-attached regions bind nuclear scaffolds and can function as ARS elements in both budding and fission yeasts. Mol. cell. Biol. **10**:5442–5454.
3. **Amati, B., L. Pick, T. Laroche, and S. M. Gasser.** 1990. Nuclear scaffold attachment stimulates, but is not essential for ARS activity in Saccharomyces cerevisiae: analysis of Drosophila ftz SAR. EMBO J. **9**:4007–4016.
4. **Arai, K.-I., S.-I. Yasuda, and A. Kornberg.** 1981. Mechanisms of dnaB protein action. J. Biol. Chem. **256**:5247–5252.
5. **Borowiec, J. A., F. B. Dean, P. A. Bullock, and J. Hurwitz.** 1990. Binding and unwinding—how T antigen engages the SV40 origin of DNA replication. Cell **60**:181–184.
6. **Borowiec, J. A., and J. Hurwitz.** 1988. Localized melting and structural changes in the SV40 origin of replication induced by T antigen. EMBO J. **7**:3149–3158.
7. **Bradly, M. K.** 1990. Activation of ATPase activity of simian virus 40 large T antigen by the covalent affinity analog of ATP, fluorosulfonylbenzoyl 5′-adenosine. J. Virol. **64**:4939–4947.
8. **Brennan, C. A., A. J. Dombroski, and T. Platt.** 1987. Transcription termination factor rho is an RNA-DNA helicase. Cell **48**:945–952.

9. **Brun, C., Q. Dang, and R. Miassod.** 1990. Studies of an 800-kilobase DNA stretch of the *Drosophila* X chromosome: comapping of a subclass of scaffold-attached regions with sequences able to replicate autonomously in *Saccharomyces cerevisiae*. Mol. Cell. Biol. **10**:5455–5465.
10. **Dean, F. B., M. Dodson, H. Echols, and J. Hurwitz.** 1987. ATP-dependent formation of a specialized nucleoprotein structure by simian virus 40 (SV40) large tumor antigen at the SV40 replication origin. Proc. Natl. Acad. Sci. USA **84**:8981–8985.
11. **Deb, S., A. L. DeLucia, C. P. Baur, A. Koff, and P. Tegtmeyer.** 1986. Domain structure of the simian virus 40 core origin of replication. Mol. Cell. Biol. **6**:1663–1670.
12. **Deb, S. P., and P. Tegtmeyer.** 1987. ATP enhances the binding of simian virus 40 large T antigen to the origin of replication. J. Virol. **61**:3649–3654.
13. **DeBruyn Kops, A., and D. M. Knipe.** 1988. Formation of DNA replication structures in herpes virus-infected cells requires a viral DNA binding protein. Cell **55**:857–868.
14. **Delucia, A. L., B. A. Lewton, R. Tjian, and P. Tegtmeyer.** 1983. Topography of simian virus 40 A protein-DNA complexes: arrangement of pentanucleotide interaction sites at the origin of replication. J. Virol. **46**:143–150.
15. **DePamphilis, M. L., and M. K. Bradley.** 1986. Replication of SV40 and polyoma virus chromosomes, p. 99–246. *In* N. P. Salzman (ed.), The Papovaviridae, vol. 1. Plenum Publishing Corp., New York.
16. **Dodson, M., F. B. Dean, P. Bullock, H. echols, and J. Hurwitz.** 1987. Unwinding of duplex DNA from the SV40 origin of replication by T antigen. Science **238**:964–967.
17. **Dornreiter, I., A. Höss, A. Arthur, and E. Fanning.** 1990. SV40 T antigen binds directly to the large subunit of purified DNA polymerase alpha. EMBO J. **9**:3329–3336.
18. **Farache, G., S. V. Razin, J. Rzeszowska-Wolny, J. Moreau, F. Recillas Targa, and K. Scherrer.** 1990. Mapping of structural and matrix attachment sites in the α-globin gene domain of avian erythroblasts and erythrocytes. Mol. Cell. Biol. **10**:5349–5358.
19. **Finger, L. R., and J. P. Richardson.** 1982. Stabilization of the hexameric form of Escherichia coli protein rho under ATP hydrolysis conditions. J. Mol. Biol. **156**:203–219.
20. **Gannon, J. V., and D. P. Lane.** 1987. p53 and DNA polymerase α compete for binding to SV40 T antigen. Nature (London) **329**:456–458.
21. **Gayama, S., T. Kataoko, M. Wachi, G. Tamura, and K. Nagai.** 1990. Periodic formation of the oriC complex of Escherichia coli. EMBO J. **9**:3761–3765.
22. **Goetz, G. S., F. B. Dean, J. Hurwitz, and S. W. Matson.** 1988. The unwinding of duplex regions in DNA by the simian virus 40 large tumor antigen-associated DNA helicase activity. J. Biol. Chem. **263**:383–392.
23. **Gurney, E. G., R. O. Harrison, and J. Fenno.** 1980. Monoclonal antibodies against simian virus 40 T antigens: evidence for distinct subclasses of large T antigen and for similarities among nonviral T antigens. J. Virol. **34**:752–763.
24. **Harper, F., Y. Florentin, and E. Puvion.** 1985. Large T antigen-rich viral DNA replication loci in SV40-infected monkey kidney cells. Exp. Cell Res. **161**:434–444.
25. **Hough, P. V. C., I. A. Mastrangelo, J. S. Wall, J. F. Hainfeld, M. Sawadogo, and R. G. Roeder.** 1987. The gene-specific initiation factor USF (upstream stimulatory factor) bound at the adenovirus type 2 major late promoter: mass and three-dimensional structure. Proc. Natl. Acad. Sci. USA **84**:4826–4830.
26. **Jones, C., and R. T. Su.** 1987. Association of viral and plasmid DNA with nuclear matrix during productive infection. Biochim. Biophys. Acta **910**:52–62.
27. **Kornberg, A.** 1982. Supplement to DNA replication. W. H. Freeman Co., San Francisco.
28. **Kornberg, A.** 1988. DNA replication. J. Biol. Chem. **263**:1–4.
29. **Lee, S.-H., T. Eki, and J. Hurwitz.** 199. Synthesis of DNA containing the simian virus 40 origin of replication by the combined action of DNA polymerases α and δ. Proc. Natl. Acad. Sci. USA **86**:7361–7365.
30. **Li, J. J., and T. J. Kelly.** 1985. Simian virus 40 DNA replication in vitro: specificity of initiation and evidence for bidirectional replication. Mol. Cell. Biol. **5**:1238–1246.

30a. **Loeber, G., P. Parsons, and P. Tegtmeyer.** 1989. The zinc finger region of simian virus 40 large T antigen. J. Virol. **63**:94–100.

31. **Mastrangelo, I. A., P. V. C. Hough, J. S. Wall, M. Dodson, F. B. Dean, and J. Hurwitz.** 1989. ATP-dependent assembly of double hexamers of SV40 T antigen at the viral origin of DNA replication. Nature (London) **338**:658–662.
32. **Maxam, A. M., and W. Gilbert.** 1977. A new method for sequencing DNA. Proc. Natl. Acad. Sci. USA **74**:560–564.
33. **Mohr, I. J., B. Stillman, and Y. Gluzman.** 1987. Regulation of SV40 DNA replication by phosphorylation of T antigen. EMBO J. **6**:153–160.
34. **Nakayasu, H., and R. Berezney.** 1989. Mapping replicational sites in the eucaryotic cell nucleus. J. Cell Biol. **108**:1–11.
35. **Parsons, R., M. E. A. Anderson, and P. Tegtmeyer.** 1990. Three domains in the simian virus 40 core origin orchestrate the binding, melting and DNA helicase activity of T antigen. J. Virol. **64**:509–518.
36. **Privalov, P. L., and S. J. Gill.** 1988. Stability of protein structure and hydrophobic interaction. J. Adv. Protein Chem. **39**:191–324.
37. **Roberts, M.** 1989. Simian virus 40 (SV40) large tumor antigen causes stepwise changes in SV40 origin structure during initiation of DNA replication. Proc. Natl. Acad. Sci. USA **86**:3939–3943.
38. **Sambrook, J., E. F. Fritsch, and T. Maniatis.** 1989. Molecular cloning, 2nd ed. Cold Spring Harbor Laboratory Press, Cold Spring Harbor, N.Y.
39. **Scheffner, M., R. Wessel, and H. Stahl.** 1989. SV40 T antigen catalysed duplex DNA unwinding. Curr. Top. Microbiol. Immunol. **144**:37–45.
40. **Scheffner, M., R. Wessel, and H. Stahl.** 1989. Sequence independent duplex DNA opening reaction catalysed by SV40 large T antigen. Nucleic Acids Res. **17**:93–106.
41. **Schiedner, G., R. Wessel, M. Scheffner, and H. Stahl.** 1990. Renaturation and DNA looping promoted by the SV40 large T antigen. EMBO J. **9**:2937–2943.
42. **Schirmbeck, R., and W. Deppert.** 1987. Specific interaction of simian virus 40 large T antigen with cellular chromatin and nuclear matrix during the course of infection. J. Virol. **61**:3561–3569.
43. **Schirmbeck, R., and W. Deppert.** 1991. Structural topography of simian virus 40 DNA replication. J. Virol. **65**:2578–2588.
44. **Smale, S. T., and R. Tjian.** 1986. T-antigen–DNA polymerase alpha complex implicated in simian virus 40 DNA replication. Mol. Cell. Biol. **6**:4077–4087.
45. **Stahl, H., M. Bauer, and R. Knippers.** 1983. The simian-virus-40 large-tumor antigen in replicating viral chromatin. A salt resistant protein-DNA interaction. Eur. J. Biochem. **134**:55–61.
46. **Stahl, H., P. Dröge, and R. Knippers.** 1986. DNA helicase activity of SV40 large tumor antigen. EMBO J. **5**:1939–1944.
47. **Stahl, H., P. Dröge, H. Zentgraf, and R. Knippers.** 1985. A large-tumor-antigen-specific monoclonal antibody inhibits DNA replication of simian virus 40 minichromosomes in an in vitro elongation system. J. Virol. **54**:473–482.
48. **Stahl, H., and R. Knippers.** 1987. The simian virus 40 large tumor antigen. Biochim. Biophys. Acta **910**:1–10.
49. **Stahl, H., M. Scheffner, M. Wiekowski, and R. Knippers.** 1988. DNA unwinding function of the SV40 large tumor antigen. Cancer Cells **6**:105–112.
50. **Stillman, B. W., and Y. Gluzman.** 1985. Replication and supercoiling of simian virus 40 DNA in cell extracts from human cells. Mol. Cell. Biol. **5**:2051–2060.
51. **Tack, L. C., and G. N. Proctor.** 1987. Two major replicating simian virus 40 chromosome classes. J. Biol. Chem. **262**:6339–6349.
52. **Tjian, R.** 1978. The binding site on SV40 DNA for a T antigen-related protein. Cell **13**:165–179.
53. **Van der Velden, H. M. W., and F. Wanka.** 1987. The nuclear matrix—its role in the spatial organization and replication of eukaryotic NA. Mol. Biol. Rep. **12**:69–77.
54. **Voelkerding, K., and D. F. Klessig.** 1986. Identification of two

nuclear subclasses of the adenovirus type 5-encoded DNA-binding protein. J. Virol. **60**:353–362.
55. **Vogelstein, B., D. M. Pardoll, and D. S. Coffey.** 1980. Supercoiled loops and eucaryotic DNA replication. Cell **22**:79–85.
56. **Vollenweider, H., J. Sogo, and T. Koller.** 1975. A routine method for protein-free spreading of double- and single-stranded nucleic acid molecules. Proc. Natl. Acad. Sci. USA **72**:83–87.
57. **Watson, J. B., and J. D. Gralla.** 1987. Simian virus 40 associates with nuclear superstructures at early times of infection. J. Virol. **61**:748–754.
58. **Wessel, R., H. Müller, and H. Hoffmann-Berling.** 1990. Electron microscopy of DNA helicase I complexes in the act of strand separation. Eur. J. Biochem. **189**:277–285.
59. **Wiekowski, M., P. Dröge, and H. Stahl.** 1987. Monoclonal antibodies as probes for a function of large T antigen during the elongation process of simian virus 40 DNA replication. J. Virol. **61**:411–418.
60. **Wiekowski, M., M. W. Schwarz, and H. Stahl.** 1988. Simian virus 40 large T antigen DNA helicase. J. Biol. Chem. **263**:436–442.